Journal of Solid State Chemistry 184 (2011) 509–515

Contents lists available at ScienceDirect

Journal of Solid State Chemistry

journal homepage: www.elsevier.com/locate/jssc

High-temperature synthesis of highly hydrothermal stable mesoporous silica and Fe–SiO_2 using ionic liquid as a template

Hong Liu [a,*], Mengyang Wang [a], Hongjiu Hu [b], Yuguang Liang [a], Yong Wang [a], Weiran Cao [a], Xiaohong Wang [c]

[a] Department of Chemical Engineering, Shanghai University, 99 Shangda Road, Shanghai 200444, PR China
[b] College of Science, Shanghai University, 149 Yanchang Road, Shanghai 200072, PR China
[c] Institute of Nano Micro Energy, Shanghai University, 99 Shangda Road, Shanghai 200444, PR China

ARTICLE INFO

Article history:
Received 17 September 2010
Received in revised form
30 December 2010
Accepted 3 January 2011
Available online 8 January 2011

Keywords:
Mesoporous
Hydrothermal stability
Ionic liquid
High temperature
Sodium fluoride

ABSTRACT

Mesoporous silicas and Fe–SiO_2 with worm-like structures have been synthesized using a room temperature ionic liquid, 1-hexadecane-3-methylimidazolium bromide, as a template at a high aging temperature (150–190 °C) with the assistance of NaF. The hydrothermal stability of mesoporous silica was effectively improved by increasing the aging temperature and adding NaF to the synthesis gel. High hydrothermally stable mesoporous silica was obtained after being aged at 190 °C in the presence of NaF, which endured the hydrothermal treatment in boiling water at least for 10 d or steam treatment at 600 °C for 6 h. The ultra hydrothermal stability could be attributed to its high degree of polymerization of silicate. Furthermore, highly hydrothermal stable mesoporous Fe–SiO_2 has been synthesized, which still remained its mesostructure after being hydrothermally treated at 100 °C for 12 d or steam-treated at 600 °C for 6 h.

1. Introduction

Mesoporous molecular sieves have attracted much attention because of their potential use as versatile catalysts and catalyst supports for the conversion of large molecules. However, as compared with conventional zeolites, these mesostructured materials have relatively low hydrothermal stability, which severely hinders their practical applications as catalysts in petroleum refining and fine chemicals synthesis. Now many efforts have been made to improve the hydrothermal stability of mesoporous materials, including the post-treatment with organosilane, incorporation of heteroatoms by doping or post-grafting, pH adjusting, assembly of zeolite precursors, and the addition of inorganic salt [1–5]. In addition, increasing the aging temperature would be also a good way to enhance the level of silica condensation and finally improve the hydrothermal stability [6]. However, the thermal stability of hydrocarbon surfactants is so low that the increased aging temperature may cause a distortion of the micelle and impact the ordering of the mesostructure, and even decompose the surfactants [7,8]. So the strategy of using higher aging temperatures for the synthesis of mesoporous materials may require special surfactants that can be used as template at high temperature. Xiao et al. [6,7] demonstrated the synthesis at high temperature (150–220 °C) and obtained hydrothermal stable mesoporous silica with a mixture of fluorocarbon and hydrocarbon surfactants as templates. Fluorocarbon surfactant has a higher thermal stability than hydrocarbon surfactant, so the mixed surfactants (fluorocarbon–hydrocarbon surfactant) may lead to high hydrothermal stability. Unfortunately, due to the rigidity and strong hydrophobicity of the fluorocarbon chains, fluorocarbon surfactants are not suitable as templates alone for the preparation of mesoporous materials [9]. Moreover, fluorocarbon surfactants are environment unfriendly.

Recently, room temperature ionic liquids (RTILs) have received considerable attentions in many areas of chemistry and industry due to their superior properties such as high thermal stability, nonflammability, negligible vapor pressure, etc. [10]. More importantly, the self-structuration of RTILs originated from the extended H-bond systems make RTILs suitable as template for the synthesis of inorganic materials with ultrafine nanostructure. For example, ordered inorganic oxides including laminar and wormlike SiO_2, mesoporous TiO_2 aggregates and hollow TiO_2 spheres, hierarchical ZnO nanostructures and hierarchical mesoporous V_2O_5 have been successfully synthesized in RTILs [11–15]. Compared to conventional templates, RTILs can be recycled more easily, which is considered to be economical and environment-friendly. In addition, the high thermal stability of ionic liquids makes it possible to perform many reactions at the higher

* Corresponding author. Fax: +86 21 66137725.
E-mail address: liuhong@shu.edu.cn (H. Liu).

0022-4596/$ - see front matter © 2011 Elsevier Inc. All rights reserved.
doi:10.1016/j.jssc.2011.01.006

temperatures, which may lead to porous materials with novel structure and properties. However, to the best of our knowledge, there is no report about the synthesis of mesoporous materials at high temperature in RTILs so far. In this paper, we report a first example of using ionic liquid as a template to synthesize highly hydrothermal stable mesoporous silica and Fe–SiO_2 at high temperature (150–190 °C) under the assistance of NaF.

2. Experimental

2.1. Synthesis of samples

The synthesis of mesoporous silicas was carried out as follows. 1.93 g RTIL, 1-hexadecane-3-methylimidazolium bromide ([C_{16}min]Br) was dissolved in 25 ml of deionized water, then 3.12 g of tetraethyl orthosilicate (TEOS) was added dropwise under vigorous stirring. The mixed solution was stirred for 1 h, then 0.063 g sodium fluoride (NaF) was added. The pH of mixture was adjusted to 9 using ammonia and stirred for 1 h. The molar composition of mixture was: 1.0 SiO_2:0.33 [C_{16}min]Br:0.10 NaF:1.58NH_4OH:100H_2O. The resulting mixture was transferred to a 100 ml Teflon-lined stainless steel autoclave at 150–190 °C for 3 d. Then the product was recovered by filtration, washed thoroughly with deionized water, and dried at 100 °C overnight. The as-synthesized material was calcined in air at 550 °C for 6 h to remove the template. Samples without the addition of NaF were also synthesized with a similar procedure.

The preparation procedure of Fe–SiO_2 sample was similar to that of the pure silica sample, except using $Fe(NO_3)_3 \cdot 9H_2O$ as a Fe source. The Fe/Si mole ratio in the solid is 0.015.

2.2. Characterization

Powder X-ray diffraction (XRD) analysis was performed on a Rigaku D/max-2400 diffractometer using Cu$K\alpha$ radiation and a graphite monochromator. Scanning electron microscopy (SEM) micrograph was obtained on a JSM-6360LV microscope. Transmission electron microscopy (TEM) images were obtained using a TECNAI 20S-TWIN electron microscope at 200 kV. Samples were prepared by evaporating very dilute suspensions onto carbon-coated grids. N_2 adsorption–desorption isotherms were obtained at −196 °C on a Micromeritics ASAP 2010 sorptometer using static adsorption procedures, and the BET surface areas and pore size distributions were calculated by using N_2 adsorption–desorption isotherms. ^{29}Si MAS NMR spectra were recorded on a Varian 400 VRX solid-state NMR spectrometer at 79.5 MHz under single-pulse mode with a 7 mm zirconia rotor, a spinning frequency of 4 kHz, pulse width of 8.5 μs, and a pulse delay of 870 s.

2.3. Hydrothermal stability evaluation

Stability in boiling water was evaluated by refluxing the samples (0.2 g) in 100 ml boiling water for different period of time.

The high-temperature hydrothermal (steam) stability was tested by treating the sample at 600 °C for 6 h in a flow of nitrogen saturated with water vapor at 100 °C.

3. Results and discussion

3.1. Influence of synthesis temperature

Fig. 1a gives the SXRD patterns of mesoporous silica synthesized at various temperatures in the absence of NaF. The calcined samples exhibit only single broad (1 0 0) diffraction peak at about $2\theta = 1$–2°, indicating the typical less long-range ordered worm-like mesoporous structure. It is similar to that of MSU-type mesoporous silica [16]. It is noted that with the increase in the aging temperature, the peak position shifts to lower angle a little bit and the pore to pore correlation distance (d_{100}) increases, which is in accord with the previous results synthesized at relatively low temperatures [9]. The diffraction intensity decreases slightly when the aging temperature increased from 150 to 190 °C, indicating the lesser ordering of the mesostructures synthesized at higher temperature, but they are still good enough.

Fig. 1b and c depict the N_2 adsorption–desorption isotherms and the corresponding BJH pore size distributions of the calcined samples. The structural properties of the samples are summarized in Table 1. It can be seen from Fig. 1b and c that all samples exhibit type IV isotherms with a typical capillary condensation step at the relative pressure (P/P_0) range of 0.3–0.6, which confirms that they are typical ordered mesoporous materials with uniform pore size. With the increase in the aging temperature, the pore size of sample decreases and the wall thickness increases (as shown in Table 1). The "thicker" silica walls obtained at higher aging temperature is attributed to the higher degree of condensation, which can be confirmed by the NMR results (Fig. 4). In addition, it is worth noting that all the samples have relatively low surface area compared to the sample synthesized at conventional lower temperatures (<120 °C). This may be due to the high density of thick walls caused by the high aging temperature [8]. But the surface area of samples synthesized with RTIL is larger than the that of samples with fluorocarbon–hydrocarbon surfactant reported by Xiao et al. [6,7] and Wang et al. [8], because the RTIL, [C_{16}min]Br is more hydrophilic than fluorocarbon.

The SEM and TEM images of the mesoporous silica synthesized at 190 °C are shown in Fig. 2. From Fig. 2a and b, it is clear that this material is composed of spherical particles of dimension 400–500 nm in diameter. The high-resolution TEM image of the sample shown in Fig. 2c reveals a disordered, wormhole mesopore structure, which is consistent with the results of small-angle XRD and N_2 adsorption–desorption. As shown in Fig. 2c, a network of channels is regular in diameter, although long-range packing order is absent.

Fig. 3 shows the XRD patterns of calcined silica samples synthesized at different temperature and the treated samples after being boiled in water at 100 °C for various times. As shown in Fig. 3, the sample synthesized at 150 °C suffers great structure loss after 3 d. However, the sample synthesized at 170 °C preserves its mesoporous structure after being boiled in water for 3 d. It suffers great structure loss after another 1 d. As for the sample synthesized at 190 °C, the mesoporous structure is well kept after 6 d and the XRD intensity does not reduce. It suffers great structure loss after 8 d. The porosity data shown as in Table 1 indicate that the BET surface area of the sample synthesized at 150 °C decrease by 65.2% after being boiled for 3 d. In contrast, the BET surface area of the sample synthesized at 170 °C merely decrease by 10.1% after this treatment. For the sample synthesized at 190 °C, there is only a 3.56% decrease in BET surface area after treatment for 6 d. The above results clearly indicate increasing the aging temperature is advantageous to the improvement of hydrothermal stability. This is attributed to the fact that the pore walls of the sample are fully condensed at relatively high temperature, which can be further confirmed by ^{29}Si MAS NMR analysis.

Fig. 4 shows the solid-state ^{29}Si MAS NMR spectra of the samples aged at different temperature, providing direct evidence of the extent of silica condensation. Two distinct resonance peaks at −99 and −112 ppm corresponding to Q^3 and Q^4, respectively, are clearly seen, whereas no Q^2 ($\delta = -92$ ppm) units are observed.

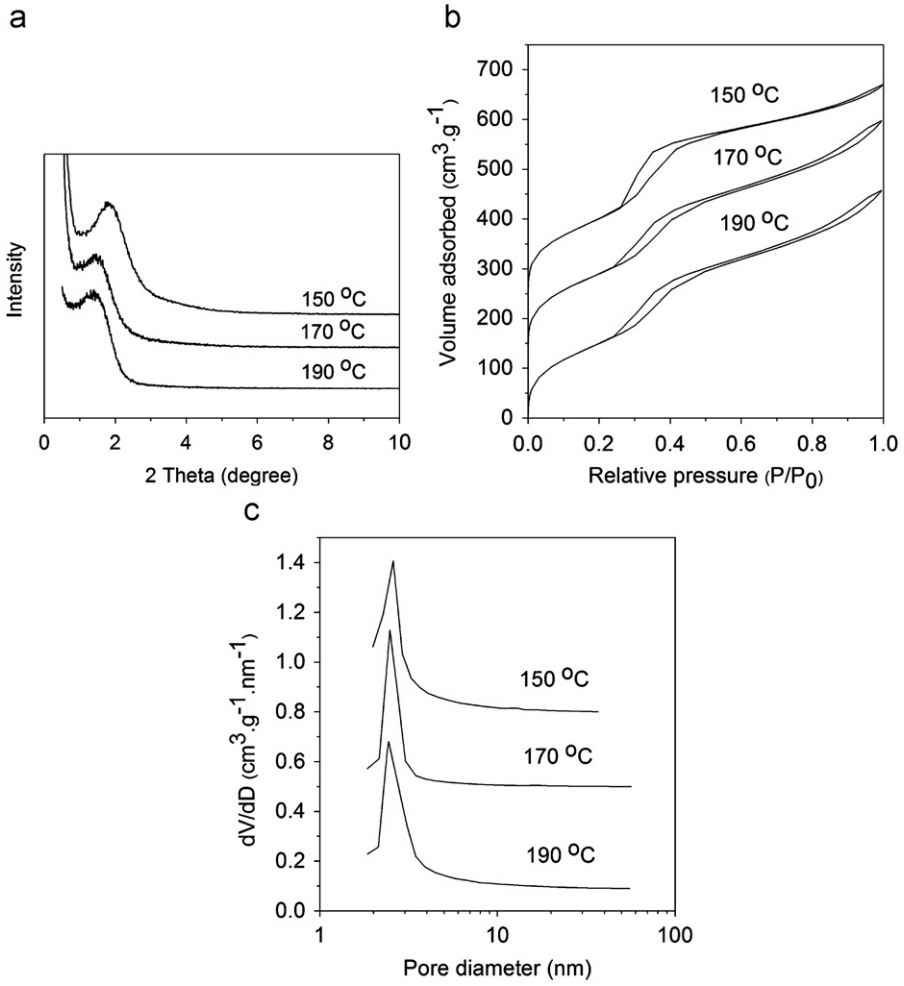

Fig. 1. XRD patterns (a), N_2 adsorption–desorption isotherms (b) and pore size distribution curves (c) of mesoporous SiO_2 synthesized at different temperatures without NaF.

Table 1
Structural properties of the calcined and hydrothermally treated mesoporous SiO_2.

Sample	d_{100} (nm)	Pore diameter (nm)	Wall thickness (nm)	S_{BET} ($m^2\ g^{-1}$)	Pore volume ($cm^3\ g^{-1}$)	S_{BET} reduced (%)	Pore volume reduced (%)	Q^4/Q^3
S150[a]	4.90	2.59	3.07	458.9	0.998			0.86
S150-boiling 3 d	4.92	2.66+18.3[c]	3.02	159.7	0.467	65.2	53.2	
S170[a]	5.58	2.48	3.96	515.5	1.272			2.91
S170-boiling 3 d	5.58	2.49	3.95	463.4	1.066	10.1	16.2	
S190[a]	5.80	2.44	4.25	507.9	1.180			4.22
S190-boiling 6 d	5.78	2.44	4.24	489.8	1.072	3.56	9.2	
S190-boiling 8 d	5.75	2.55+17.7[c]	4.08	246.4	0.646	51.5	45.3	
S190F[b]	5.78	2.42	4.26	505.3	1.127			5.20
S190F-boiling 10 d	5.76	2.42	4.23	461.7	1.054	8.6	6.5	
S190F-steaming 6 h	5.76	2.46	4.19	432.6	0.979	14.4	13.1	

[a] Synthesized without NaF.
[b] Synthesized with NaF.
[c] Pores come from the aggregation of particles (void space).

Here Q^n represents Si in different coordination environments of $Si(OSi)_n(OH)_{4-n}$ and $n=2$–4 [17]. The relative integrated intensities of the Q^4/Q^3 signals increase with the aging temperature (Fig. 4), and the ratio of Q^4/Q^3 increases from 0.86 (150 °C) to 4.22 (190 °C) (Table 1). The above result implies that the high aging temperature can enhance silicate condensation and favors the formation of mesoporous materials with more completely cross-linked frameworks.

3.2. Influence of NaF

Fig. 5 shows XRD patterns of calcined and hydrothermally treated samples synthesized at 190 °C with and without NaF. The sample without the aid of fluoride ion loses the mesoporous structure after hydrothermal treatment for 8 d. However, the sample synthesized with the aid of fluoride ion still preserves its mesoporous structure after being boiled in water for 10 d.

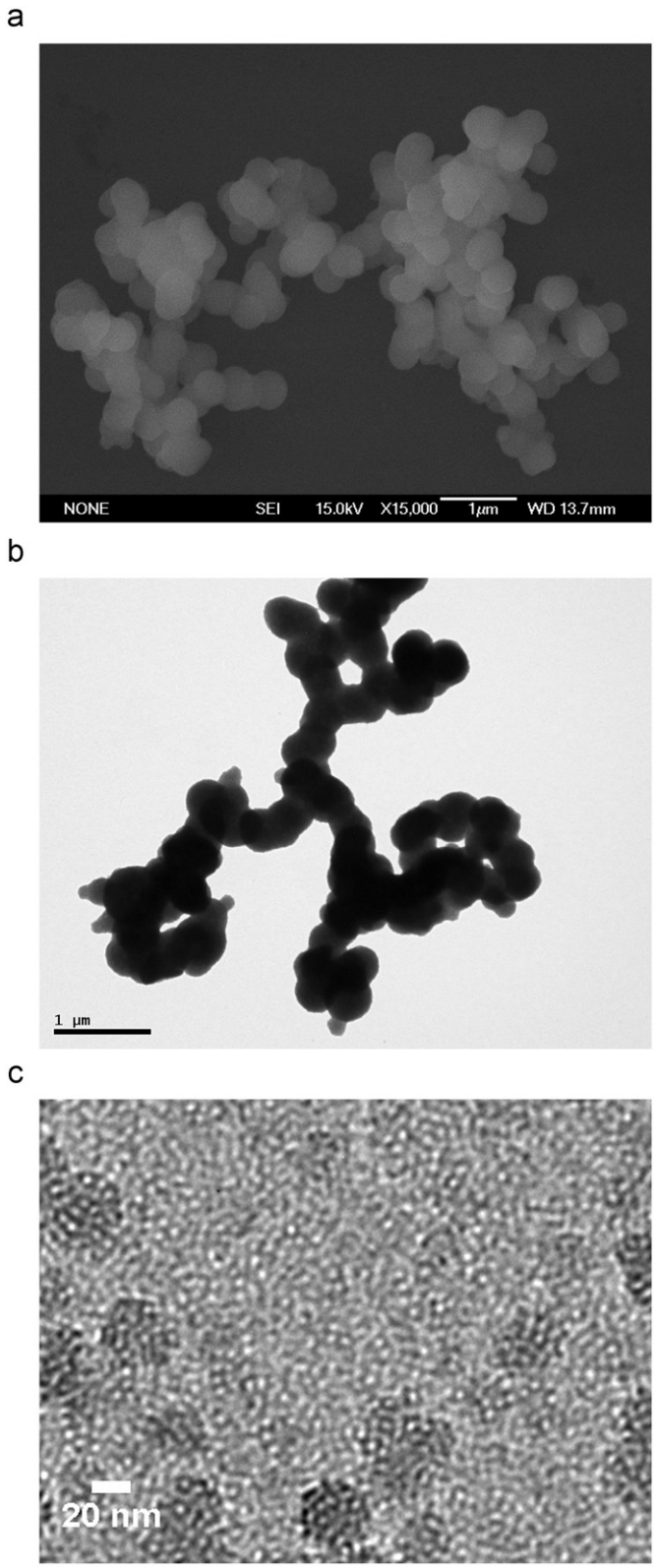

Fig. 2. SEM (a), low-resolution (b) and high-resolution (c) TEM images of the mesoporous SiO_2 synthesized at 190 °C without NaF.

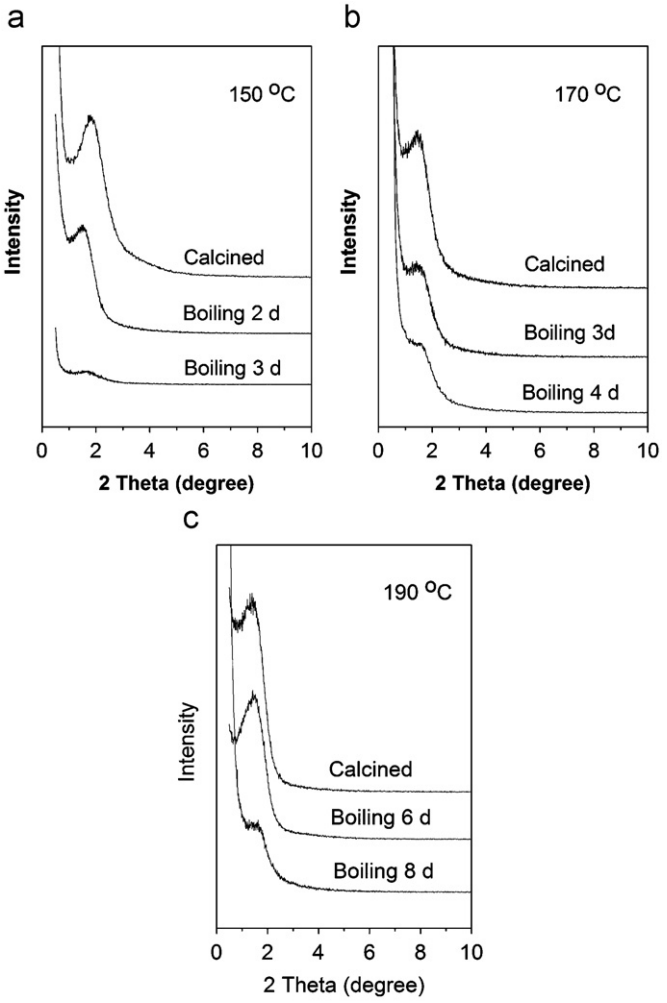

Fig. 3. XRD patterns of mesoporous SiO_2 after being treated in boiling water.

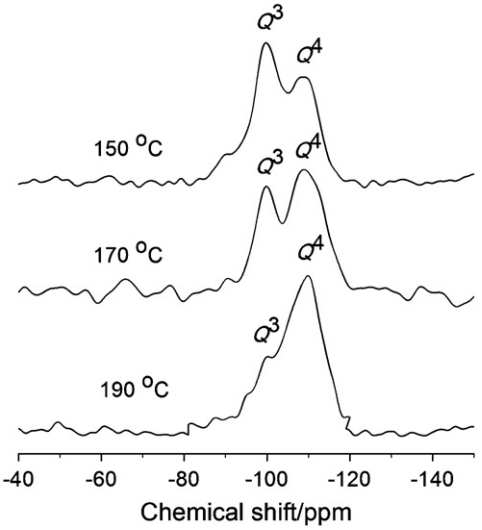

Fig. 4. ^{29}Si MAS NMR spectra of mesoporous SiO_2 synthesized at different temperatures without NaF.

And there are no significant changes in 2θ positions, peak intensities, and linewidths compared with those of calcined sample. These results indicate the addition of fluoride ion can drastically enhance the hydrothermal stability of mesoporous silica. To assess the high-temperature hydrothermal stability, the SXRD pattern of steam-treated (600 °C, 6 h) sample synthesized at 190 °C with NaF is also displayed in Fig. 5. The pattern also shows a very intense (1 0 0) diffraction peak, which means that the mesostructures are not destroyed even under such severe

conditions. This result demonstrates that the sample synthesized at 190 °C with NaF has remarkable hydrothermal stability.

Fig. 6 shows the N_2 adsorption–desorption results of calcined and hydrothermally treated samples synthesized at 190 °C with and without NaF. After being treated in boiling water for 8 d, the pore structure of the sample without NaF is already degraded, as reflected in the disappearance of the capillary condensation step in the N_2 isotherm. The material suffers a 51.5% decrease in BET surface area (Table 1). Whereas, the N_2 adsorption–desorption results of the sample synthesized with NaF indicate that after being treated in boiling water for 10 d or steam-treated for 6 h, the sample still exhibits type IV isotherm and possess a uniform pore size distribution. According to the data presented in Table 1, the treated sample maintains most of the BET surface area and pore volume. There is only an 8.6% decrease in the BET surface area after hydrothermal treatment in boiling water for 10 d and a 14.4% decrease after steam treatment. All of the results further demonstrate that the sample synthesized with NaF has remarkable hydrothermal stability.

Fig. 7 shows the ^{29}Si MAS NMR spectra of calcined samples synthesized with and without NaF. It is obvious that the sample with addition of fluoride has the higher Q^4/Q^3 ratio than the sample without fluoride, indicating that addition of fluoride ions can enhance the polymerization degree of silicates. It is attributed to the addition of NaF can increase the interaction between surfactant headgroups and the silicon precursor by additive electrolyte effect, thus promote the formation and growth of mixed micelle, enhance self-assembly of micelles, boost the arrangement of the channels, accelerate the hydrolysis and condensation of the silicon precursor [18,19]. The Q^4/Q^3 ratio for the sample with addition of fluoride is 5.20 (Table 1), indicating the fully condensed walls of this sample. The higher silicate condensation degree indicates fewer defects in the framework, which can more easily resist the water attack and are responsible for the higher hydrothermal stability. In addition, the addition of fluoride will also lead to the formation of Si–F bonds and a decrease of hydroxyl groups on silica oligomers. Because the binding energy of Si–F bonds is larger than that of Si–O bonds, it is

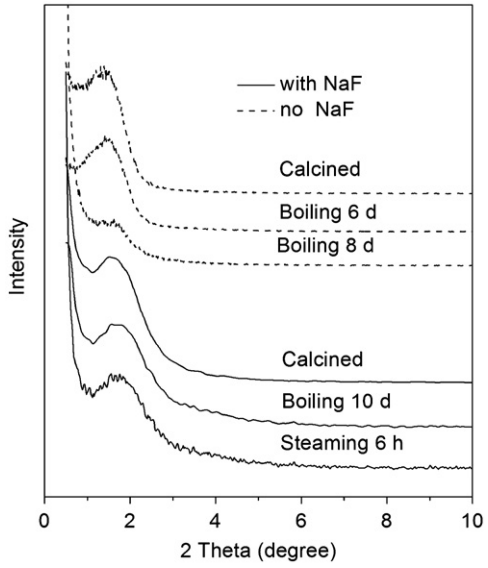

Fig. 5. XRD patterns of the calcined and hydrothermally treated mesoporous SiO_2 synthesized at 190 °C.

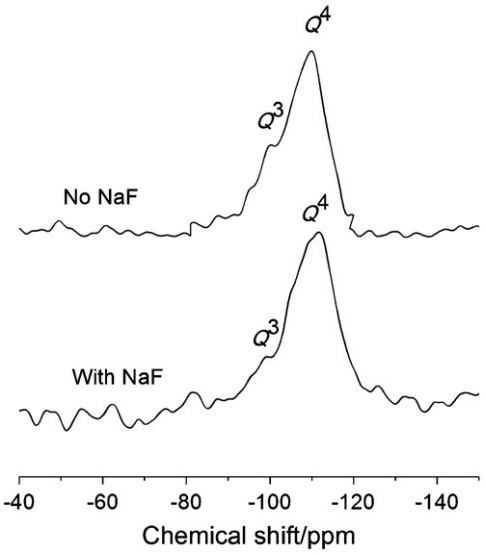

Fig. 7. ^{29}Si MAS NMR spectra of mesoporous silica synthesized with and without NaF.

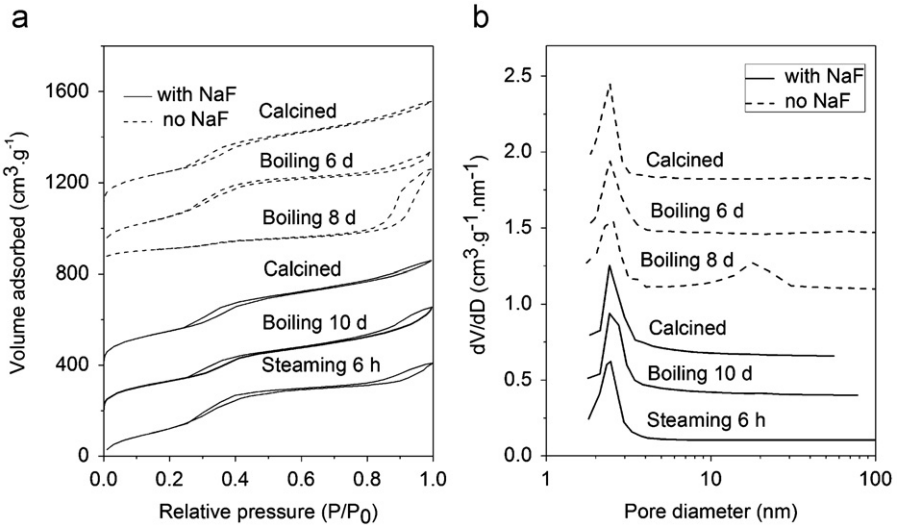

Fig. 6. Nitrogen adsorption–desorption isotherms (a) and pore size distribution curves (b) of the calcined and hydrothermally treated mesoporous SiO_2 synthesized at 190 °C.

difficult for Si–F to be broken. These "tough" bonds on the pore surface lead to the natural resistance of the fluorinated surface to the hydrolysis by water molecules [18], which is also the reason for improvement of the hydrothermal stability of mesoporous material.

3.3. Synthesis of high hydrothermal stable Fe–SiO_2

The above method also can be extended to the synthesis of iron-incorporated mesoporous silica. The preparation procedure of Fe–SiO_2 sample is similar to that of the pure silica sample, except using $Fe(NO_3)_3 \cdot 9H_2O$ as a Fe source. The Fe/Si mole ratio in the solid is 0.015. Fig. 8a shows that the mesostructures of the Fe–SiO_2 sample are still maintained after being treated in boiling water for 12 d or steam-treated for 6 h.

The N_2 adsorption–desorption isotherms and the corresponding pore size distribution of Fe–SiO_2 and the hydrothermal treated sample are given in Fig. 8b and c. After being treated in boiling water or steam-treated for 6 h, the sample still exhibits type IV isotherm and possess a slightly broadened pore size distribution. The specific structural parameters are given in Table 2. It can be seen that there is only an 11.9% decrease in BET surface area after treatment in boiling water for 12 d and a 13.3% decrease after steam treatment. It is notable that the mesoporous Fe–SiO_2 molecular sieve exhibits much better hydrothermal stability than the pure silica sample synthesized at high temperature. It is generally accepted that structural degradation of pure silica materials by molecular water occurs by hydrolysis of Si–O–Si bonds. During the synthesis of Fe–SiO_2, the Fe is attached to or incorporated into the silica framework and form the Si–O–Fe bonds, which are more stable to attack from water than Si–O–Si bonds. Thus, the Fe–SiO_2 material generally exhibits significant enhancement of hydrothermal stability. Similar results have been reported by Shen and Kawi [20] and Xia and Mokaya [2] in their

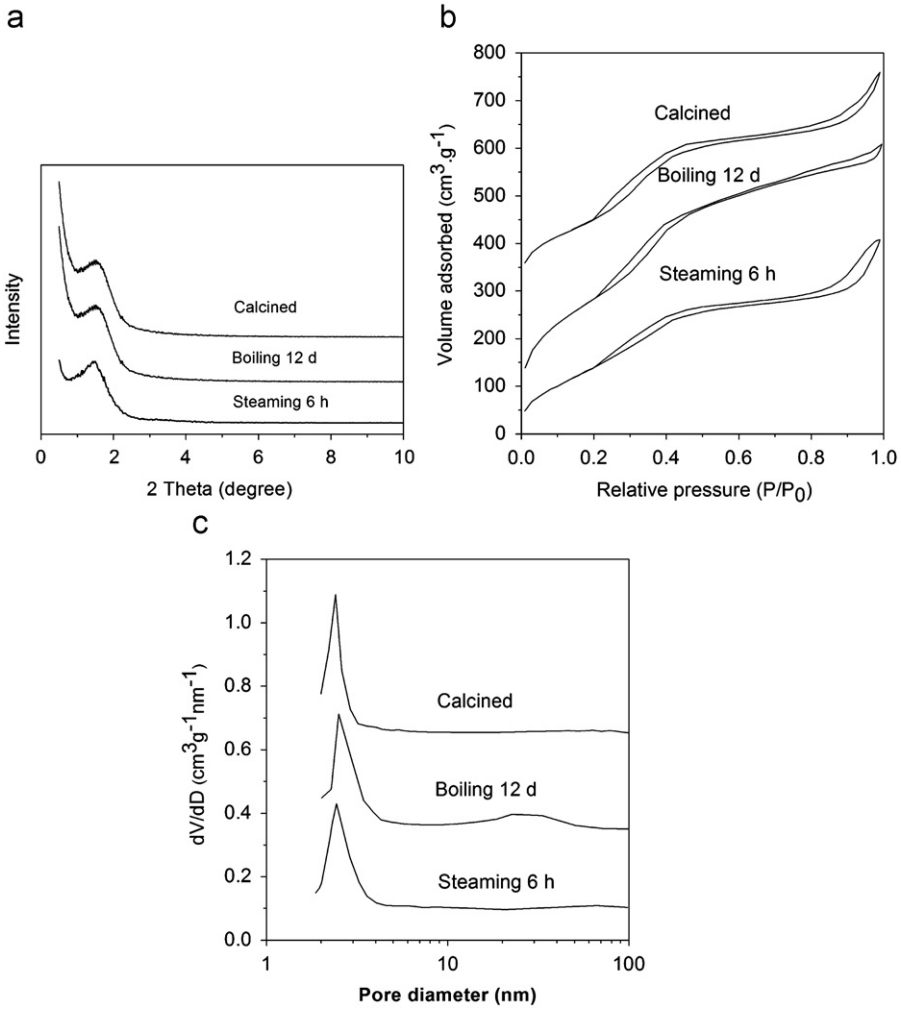

Fig. 8. XRD patterns (a), N_2 adsorption–desorption isotherms (b) and pore size distribution curves (c) of the calcined and hydrothermally treated mesoporous Fe–SiO_2.

Table 2
Structural properties of the calcined and hydrothermally treated mesoporous Fe–SiO_2 synthesized at 190 °C with NaF.

Sample	d_{100} (nm)	Pore diameter (nm)	Wall thickness (nm)	S_{BET} ($m^2\,g^{-1}$)	Pore volume ($cm^3\,g^{-1}$)	S_{BET} reduced (%)	Pore volume reduced (%)
Calcined	5.78	2.40	4.27	501.4	1.114		
Boiling 12 d	5.78	2.50	4.17	441.8	0.987	11.9	11.4
Steaming 6h	5.79	2.43	4.25	434.7	0.981	13.3	11.9

study on the hydrothermal stability of MCM-41 and MCM-48, they suggested that Al incorporated in the MCM-41 and MCM-48 framework helped to protect mesoporous framework from hydrolysis.

4. Conclusions

In conclusion, highly hydrothermal stable mesoporous silicas and Fe–SiO_2 with worm-like structures have been synthesized in a simple procedure using an ionic liquid, [C_{16}mim]Br as template under the assistance of NaF at high temperature. The combination of high aging temperature and salt effect favors the formation of mesoporous materials with more completely cross-linked frameworks, which have higher hydrothermal stability. It is expected that the present method can be easily extended to fabricate many other mesoporous materials.

Acknowledgment

This study is supported financially by Shanghai Municipal Commission of Education (No. 11YZ15) and Shanghai Leading Academic Disciplines (No. S30109).

References

[1] K.A. Koyano, T. Tatsumi, Y. Tanaka, S. Nakata, J. Phys. Chem. B 101 (1997) 9436–9440.
[2] Y.D. Xia, R. Mokaya, Microporous Mesoporous Mater. 74 (2004) 179–188.
[3] R. Ryoo, S. Jun, J. Phys. Chem. B 101 (1997) 317–320.
[4] Z.T. Zhang, Y. Han, L. Zhu, R.W. Wang, Y. Yu, S.L. Qiu, D.Y. Zhao, F.S. Xiao, Angew. Chem. Int. Ed. 41 (2002) 2226.
[5] S. Jun, J.M. Kim, R. Ryoo, Y.S. Ahn, M.H. Han, Microporous Mesoporous Mater. 41 (2000) 119–127.
[6] Y. Han, D.F. Li, L. Zhao, J.W. Song, X.Y. Yang, N. Li, Y. Di, C.J. Li, S. Wu, X.Z. Xu, X.J. Meng, K.F. Lin, F.S. Xiao, Angew. Chem. Int. Ed. 42 (2003) 3633–3637.
[7] D.F. Li, Y. Han, J.W. Song, L. Zhao, X.Z. Xu, Y. Di, F.S. Xiao, Chem. Eur. J. 10 (2004) 5911–5922.
[8] C.L. Li, Y.Q. Wang, Y.L. Guo, X.H. Liu, Y. Guo, Z.G. Zhang, Y.S. Wang, G.Z. Lu, Chem. Mater. 19 (2007) 173–178.
[9] X.J. Meng, Y. Di, L. Zhao, D.Z. Jiang, S. Li, F.S. Xiao, Chem. Mater. 16 (2004) 5518–5526.
[10] T. Welton, Chem. Rev. 99 (1999) 2071–2083.
[11] Y. Zhou, M. Antonietti, Adv. Mater. 15 (2003) 1452–1455.
[12] Y. Zhou, M. Antonietti, J. Am. Chem. Soc. 125 (2003) 14960–14961.
[13] T. Nakashima, N. Kimizuka, J. Am. Chem. Soc. 125 (2003) 6386–6387.
[14] H.G. Zhu, J.F. Huang, Z.W. Pan, S. Dai, Chem. Mater. 18 (2006) 4473–4477.
[15] H.T. Liu, P. He, Z.Y. Li, D.Z. Sun, H.P. Huang, J.H. Li, G.Y. Zhu, Chem. Asian J. 1 (2006) 701–706.
[16] S.A. Bagshaw, E. Prouzet, T.J. Pinnavaia, Science 269 (1995) 1242–1244.
[17] L.Y. Chen, T. Horiuchi, T. Mori, K. Maeda, J. Phys. Chem. B 103 (1999) 1216–1222.
[18] L.Z. Wang, J.L. Zhang, F. Chen, M. Anpo, J. Phys. Chem. C 111 (2007) 13648–13651.
[19] S.A. Bagshaw, Chem. Commun. (1999) 1785–1786.
[20] S. Shen, S. Kawi, Langmuir 18 (2002) 4720–4728.